

**Amine-functionalized mesoporous silica. A material capable of CO<sub>2</sub> adsorption  
and fast regeneration by microwave heating**

**Hakan Nigar**

Nanoscience Institute of Aragon and Chemical and Environmental Engineering  
Department, University of Zaragoza, 50018 Zaragoza, Spain

**Reyes Mallada\*, Jesus Santamaría\***

Nanoscience Institute of Aragon and Chemical and Environmental Engineering  
Department, University of Zaragoza, 50018 Zaragoza, Spain  
Networking Research Centre CIBER-BBN, 28029 Madrid, Spain

**Beatriz Garcia-Baños, Felipe L. Peñaranda-Foix, Jose M. Catalá-Civera**

Instituto ITACA, Universidad Politecnica de Valencia, Camino de Vera, 46022,  
Valencia, Spain

\*Corresponding authors: [rmallada@unizar.es](mailto:rmallada@unizar.es), [jesus.santamaria@unizar.es](mailto:jesus.santamaria@unizar.es)

The surface of ordered mesoporous (MCM-48) silica has been subjected to covalent grafting with silane molecules containing one to three amino groups. The dielectric properties of the materials were studied in detail, and the functionalized materials were used for CO<sub>2</sub> adsorption at room temperature, followed by regeneration under either conventional heating or microwave irradiation. It has been found that, as the intensity of functionalization with amino groups increases (from mono to tri-amino silanes) both the CO<sub>2</sub> load and the dielectric response at microwave frequencies increase. In particular, functionalization with a tri-amino silane derivative gave the highest CO<sub>2</sub> adsorption and the fastest microwave heating, resulting in a 4-fold acceleration of adsorbent regeneration. The grafted material was fully stable for at least 20 adsorption-regeneration cycles, making it an ideal candidate for microwave-swing adsorption (MWSA) processes.

## Introduction

Among CO<sub>2</sub> capture technologies, adsorption is the most promising in the range of low temperature operation<sup>1</sup> including post-combustion capture systems as well as the capture of CO<sub>2</sub> from ambient air its subsequent reutilization as part of a climate change mitigation strategy.<sup>2</sup> Apart from the more classical zeolites and activated carbons, in recent years metal organic frameworks (MOF), and a wide variety of amino-functionalized materials have shown exciting performance in terms of loading capacity and selectivity towards CO<sub>2</sub> adsorption. At a low CO<sub>2</sub> pressure of 0.1 kPa and 293 K the highest load around 6 mmol/g (26 %wt.) has been obtained with Mg-MOF74.<sup>3</sup> However, it is important to note that this material is hydrophilic and in the presence of water its capacity is strongly reduced, this behavior also observed for most zeolites. Appropriate functionalization of adsorbents (typically by amino groups) can also be used to increase the capacity and selectivity towards CO<sub>2</sub> adsorption. In the group of amine modified mesoporous silicas, the best results were reported by the group of Sayari et al.<sup>4,5</sup> They synthesized a pore-expanded mesoporous silica (PE-MCM41) and modified it with a tri-amine silane agent. The CO<sub>2</sub> uptake at 0.1 bar and 298 K was 2.2 mmol/g (9.7 %wt.), comparable to that of a typical zeolite 13X. However, in this case the presence of water increased the CO<sub>2</sub> uptake increases (2.9 mmol/g) outperforming the zeolite.

At least as important as the capacity and selectivity of a sorbent towards CO<sub>2</sub> is the possibility of economic regeneration. Ideally, desorption processes would be fast (to produce a concentrated CO<sub>2</sub> stream) and would require a minimal amount of energy. In fact, energy costs often determine the viability of the entire process,<sup>6</sup> which has prompted an intense research into alternative methods of energy management. In the last two decades microwave (MW) irradiation, has emerged as a highly effective

way to supply energy in several types of intensified processes<sup>7</sup> including those involving solid materials<sup>8,9</sup> such as sintering and ceramic processing<sup>10</sup>, catalysis<sup>11</sup> and desorption<sup>12</sup> in the so called Microwave Swing Adsorption, MWSA process. The main advantage of MWSA relate to the fact that, unlike conventional heating where solids heat through conduction and convection, microwaves are able to provide energy to susceptible materials in a direct manner, and thus MWs can achieve the volumetric heating of adsorbent materials when they are capable of absorbing the microwave energy. Alternatively, the use of MWs may allow for direct transfer of the energy to the adsorbate without being absorbed by the adsorbent.<sup>13</sup> There is also the possibility of selective targeting of the surface itself or of its functional groups to promote microwave desorption processes.<sup>6</sup>

Widely employed MW-heatable microporous sorbents include zeolites (or zeotypes) as polar sorbents, and activated carbon as non-polar sorbents. These two classes of materials are the only ones studied so far in MWSA, being the carbon family the most frequently used. Carbon materials are good microwave absorbers as a consequence of the interactions of the delocalized  $\pi$ -electrons with the MWs, thus converting MW energy into heat.<sup>14,15</sup> In the case of zeolites, a different heating mechanism has been found<sup>16-19</sup> related to the interaction of the electromagnetic field with, i) the water or polar molecules adsorbed in the pores, ii) the hydroxyl groups on the surface and iii) the cation movement in the structure.

The ability of a material to be heated in the presence of the MW field is defined by its dielectric loss tangent:  $\tan\delta=\epsilon''/\epsilon'$ . In turn, the dielectric loss tangent is composed of two parameters, the dielectric constant (or real permittivity),  $\epsilon'$ , and the dielectric loss factor (or imaginary permittivity),  $\epsilon''$ ; i.e.,  $\epsilon=\epsilon'-i\epsilon''$ , where  $\epsilon$  is the complex permittivity. The dielectric constant ( $\epsilon'$ ) determines the electric energy

storage in the dielectric, while the dielectric loss factor ( $\epsilon''$ ) measures the dissipation of electric energy in form of heat within the material.<sup>9</sup> The measurement of dielectric properties in solids is a difficult task, since many parameters influence the dielectric properties, in particular the frequency, the humidity, the density of the solid bed and specially the temperature play an important role.

Catala-Civera et al.<sup>20</sup> reported that, the dynamic measurement of dielectric properties of materials simultaneously with the application of MW heating at high temperatures ( $>1000^{\circ}\text{C}$ ). This report can also help to better understanding, the interactions that take place during MW heating in comparison with conventional heating techniques. Understanding the microwave heating behavior of materials may also lead us to the most effective way of transferring the energy directly to the processed materials. With proper understanding, many technically important materials can be heated in a more rapid, uniform, selective, lower cost and controlled form than is possible with conventional methods.<sup>8</sup>

Heat-driven regeneration modes, such as Temperature Swing, TS, and Temperature Swing Vacuum, TSV, are preferentially employed for the regeneration of amine-containing sorbents due to the chemical  $\text{CO}_2$ -sorbent interactions. However with these procedures the main drawback is that under conventional heating the temperature rise of the solid is slow and rapid cycling cannot be implemented.<sup>21</sup> This problem could be solved using the volumetric and selective heating afforded by microwaves. In a previous work of our laboratory, we showed a reduction in desorption time of 75% using MW-heatable zeolites as sorbents of n-hexane.<sup>19</sup> On the other hand, the desorption of  $\text{CO}_2$  by microwaves from zeotypes (zeolite X and ETS-10)<sup>6,22</sup> and carbon<sup>23</sup> has been recently reported. The promising results of these works suggest that MW heating could overcome some of the main challenges in  $\text{CO}_2$  capture

which include affordable production of a high-purity CO<sub>2</sub> stream (high adsorption/desorption rates, low energy consumption) while preserving the textural characteristics of the sorbents<sup>6</sup> to an extent that would allow their multiple reuse.

In a previous work, we synthesized a mesoporous silica MCM-48 and established the optimal conditions for functionalization with a mono-amine group.<sup>24</sup> This material showed an excellent efficiency for CO<sub>2</sub> removal at low partial pressures (0.5 mmol CO<sub>2</sub>/mol N at 5 kPa), although sorbent regeneration by MW was not explored. In the present work, we have modified the same MCM-48 with silane agents containing one, two and three amino groups to increase the CO<sub>2</sub> uptake, and we have also investigated the effect of these functionalizations have on the MW absorption properties of the solid, for MWSA operation.

In addition to studying the adsorption of CO<sub>2</sub> on mesoporous silica functionalized with different amino groups, this study will cover two important aspects in the successful design CO<sub>2</sub> MWSA processes, i.e., i) the study of the dielectric properties of the materials and ii) the regeneration process itself when carried out under microwave irradiation with especial focus on the regeneration rates achieved. Understanding MW-heating behavior of materials ultimately involves correlating dielectric properties with surface chemistry. The study will include the comparison with conventional electrical heating and the study of the stability of the sorbents after several regeneration cycles under MW-heating. In spite of the considerable potential of MWSA processes for CO<sub>2</sub> management, these aspects have been scarcely studied.<sup>22,25</sup>

## Experimental

### *Mesoporous silica MCM-48 synthesis*

A hydrothermal method was used for the synthesis of the MCM-48 with the following molar gel composition: 1.4 SiO<sub>2</sub>: 1.0 CTABr : 0.35 Na<sub>2</sub>O : 5.0 EtOH : 140 H<sub>2</sub>O. Ludox AS40 (40% SiO<sub>2</sub> : 60% H<sub>2</sub>O, Sigma-Aldrich) was used as a silica source, CTABr (hexadecyltrimethylammonium bromide, Sigma-Aldrich) as a structure-directing agent and EtOH (Absolute, Sigma-Aldrich) as an additive for the mesophase control. Two different solutions were prepared. For the silica source solution, Ludox was added slowly drop-by-drop into an aqueous solution of 1 M NaOH under vigorous stirring, this mixture was heated up to 343 K for 1 h and then the solution was cooled to room temperature. To prepare the surfactant solution, CTABr was dissolved slowly in an EtOH/H<sub>2</sub>O mixture under gently stirring to avoid the formation of bubbles. The silica solution was added drop-by-drop into the surfactant solution and stirred for 1 h. The prepared gel with a total amount of 70 g was divided in two Teflon-lined stainless steel autoclaves and subjected to hydrothermal synthesis at 373 K in a preheated oven for 4 days. Then the solid product was filtered (medium flow rate disc filter, PRAT-DUMAS), washed with hot water and dried overnight. For the elimination of the surfactant, the solid product was calcined at 813 K with a heating rate of 1 K/min in air for 6 h.<sup>24</sup>

### *Amine functionalization*

The mono-, di-, and tri-amine silane agents (see Figure 1b ) used for grafting were 3-triethoxysilylpropylamine (98%), [3-(2-aminoethylamino)propyl]trimethoxysilane (97%), and 2-[2-(3-trimethoxysilylpropylamino)ethylamino]ethylamine (technical grade), respectively, and supplied from Sigma-Aldrich. For dry grafting, 300 mg of MCM-48 powder was dispersed in 15 mL of dry toluene in a 250 mL twin-neck

round-bottom flask under continuous stirring (400 rpm) in an Argon atmosphere during 15 min., then the flask was immersed in a temperature controlled oil bath, when the mixture reached to 383 K, 650  $\mu$ L of the amine silane agent were added into the flask and stirred for 1 h under reflux. Then the solid product was vacuum filtered and washed with dichloromethane/diethyl ether (1:1) mixture and dried at 323 K for 12 h. Amine functionalized MCM-48 samples were designated as MCM-48 mono-, MCM-48 di-, MCM-48 tri.

#### *Adsorption-Desorption Experiments*

Adsorption – Desorption experiments were performed in an experimental setup previously described<sup>19</sup> which consisted of three mass flow controllers, two automatic 4-way valves and an on-line quadrupole mass spectrometer (OMNistar), MS, for the analysis of the gases. The experimental system was computer-controlled by a Labview customized program. Two different pure (99.9999%, Praxair) gases and mixtures thereof containing CO<sub>2</sub> for adsorption or N<sub>2</sub> for regeneration were fed to the bed at a total flow rate of 100 sccm. Adsorption experiments were done at 298 K and 1 bar with a 15 % concentration of CO<sub>2</sub> in a fixed-bed in a quartz tube (200 mg, 50-150  $\mu$ m, L=10 mm,  $\varnothing_{in}$ =7 mm). Prior to the adsorption runs, the sample was regenerated thermally while passing N<sub>2</sub> through the bed. Regeneration was carried out either by conventional heating with an electrical oven or by microwave heating. The microwave system (Sairem Iberica, see Figure 1 supplementary information) consists of a solid state microwave generator at 2.43 to 2.47 GHz with a maximum power of 150 W and a TE10 mode microwave cavity (Sairem) with a WR340 waveguide. The cavity was adjusted to reduce the reflected power below 5% by changing the frequency. The reflected power was measured with a Network Analyzer (Agilent E5061B 5 Hz – 3 GHz).

### *Temperature measurements*

The temperature in the fixed-bed was measured with an optical fiber (range: 193-523 K, Ø:1 mm, Neoptix) inside a capillary quartz tube located in the center of the fixed-bed.

To have a direct and accurate comparison of the heating rates obtained with different degrees of amination slabs consisting of a mixture (2:1) of KBr (material transparent to MW radiation) and the specific adsorbent were prepared. The slabs were located within the waveguide in front of one of the sampling windows to allow direct measurement of the temperature of the surface using an infrared thermographic camera (range: 273-873 K, InfraTec, GmbH). A scheme is provided in Figure 7.

### *Characterization techniques*

X-ray diffraction analyses were carried out using a Philips X'Pert MPD diffractometer with  $\text{CuK}\alpha$  radiation. The diffraction data were recorded in the  $2\theta$  range of  $0.6\text{--}6.5^\circ$  with a scanning rate of 5 s/step (step  $2\theta=0.02$ ).

Nitrogen adsorption isotherms were measured at 77 K on Micromeritics TriStar 3000 analyzer. Non-functionalized MCM-48 samples were degassed under vacuum at 473 K for 8 h, and the mono-, di- and tri-amine functionalized MCM-48 samples were degassed at 383 K for 10 h. BET surface areas were calculated using the BET equation in the linear range and pore volume was calculated at a relative pressure of 0.95. Pore size was analyzed with the software developed by Micromeritics based on Density Functional Theory, DFT. In particular for the analysis of mesoporous silicas the selected model to fit the experimental isotherm was the DFT- $\text{N}_2$  model, based on a cylindrical pore model with oxide surface.<sup>26</sup>

CO<sub>2</sub> adsorption isotherms of the different samples were measured at 298 K on Micromeritics ASAP 2020 analyzer; fixed amounts of CO<sub>2</sub> were dosed to the sample till the equilibrium pressure was achieved.

TEM images were obtained with a transmission electron microscope FEI TECNAI T20, working at 200 kV. This microscope belongs to the Laboratory of Advanced Microscopies, LMA, in the installations at the Institute of Nanoscience of Aragon (INA), University of Zaragoza..

Thermogravimetric analysis (TGAQ5000 TA instruments with a heating rate 5 K/min up to 1073 K under airflow ) was used to obtain the amount of N in the samples, using the weight loss between 403 and 1073K. This method was validated in our previous publication<sup>24</sup> by checking its results against those of standard methods such as the so-called fluorescamine method that evaluates the amount of amino groups based in reaction of the non-fluorescent fluorescamine with the primary amines, that yields a fluorescent derivative. From the total weight loss between 403 K and 1073 K the amount of N was calculated using the equivalence of 69, 49 and 47 mg of weight loss per mmol of N, for the mono-, di- and tri- functionalized samples respectively.

Fourier transform infrared (FTIR) spectroscopy of the fresh samples (not dehydrated) was performed with a Bruker Vertex 70 FTIR spectrometer equipped with a DTGS detector and a Golden Gate diamond ATR accessory. Spectra were recorded by averaging 100 scans in the 4000–600 cm<sup>-1</sup> wave number range at a resolution of 2 cm<sup>-1</sup>. Data evaluation was carried out by OPUS software from Bruker Optics.

### *Dielectric Properties*

Dielectric properties ( $\epsilon'$  and  $\epsilon''$ ) of the selected samples as a function of the temperature were measured in a microwave resonant cavity around the frequency of 2.45 GHz.<sup>20</sup> The methodology is based on the dynamic measurement of the

microwave cavity parameters as the resonant frequency and quality factor while with the sample is being heated also with microwave energy. The heating of the sample in the cavity modify the resonance properties of the microwave cavity and these changes are measured to quantify the dielectric properties as a function of the temperature. An automatic procedure adjusts dynamically the microwave power deliver to the microwave cavity to obtain the desired heating rate in the sample. The sample temperature is continuously measured with an infrared pyrometer (Optris, LT-CF2). Powders were placed in a cylindrical quartz vial ( $L=15$  mm,  $\varnothing_{in}=12$  mm), manually compacted to obtain a constant bed density, and immersed inside the cavity in a  $N_2$  atmosphere. The heating rate was adjusted to a standard rate of  $10^\circ\text{C}/\text{min}$ .

## **Results and Discussion**

### *Characterization of pristine mesoporous silica MCM-48*

Thirteen different batches of MCM-48 were synthesized as described above and characterized by  $N_2$  adsorption (as shown in Table 1, Supplementary Info) and TEM. All the samples, except one, show the same Type IV isotherm with a good reproducibility giving average  $1287\pm 93$   $\text{m}^2/\text{g}$  BET surface area and  $1.011\pm 0.007$   $\text{cm}^3/\text{g}$  pore volume and pore size analyzed by DFT of 3.5 nm, which agrees well with the values measured in the TEM images where the arrangement of the pores could be observed, see Figure 2. The XRD diffraction pattern of a representative MCM-48 sample is presented in the bottom curve of Figure 3. It shows the typical cubic structure (see Figure 1a)) indexed in the space group Ia3d. The sharp and high diffraction peaks, indicate the formation of well-ordered mesoporous material.<sup>27</sup>

### *Characterization of mono-, di-, tri-amine functionalized MCM-48 sorbents*

The above-described MCM-48 material was functionalized with different silane coupling agents, as schematized in Figure 1. The silane agent is covalently bonded to the hydroxyl groups in the silica support through alkyl-silyl linkages, see Figure 1b-c. As a consequence, the textural properties of the functionalized samples are considerably different from the pristine MCM-48 material, as shown by the N<sub>2</sub> isotherms and pore size distributions presented in Figure 4a,b (main characterization data are summarized in Table 1). MCM-48 shows a typical reversible type IV adsorption isotherm (Figure 4a), which is characteristic of mesoporous materials. With successive functionalization, the surface area and the pore volume are significantly reduced compared to the non-functionalized MCM-48. This effect is more dramatic in the case of the MCM-48-di and MCM-48-tri where bigger silane molecules were grafted (see dimensions in Figure 1b). Thus, for the case of the MCM-48-tri sample, the surface area has been reduced to about one third of the initial BET surface, and the pore volume to about one fourth. At the same time, the pore size progressively decreases from 3.5 nm in the pristine material to about 2.5 nm in the MCM-48-tri sample. The amine loading based on the TGA analyses (see Figure 2 supplementary information) increases strongly for the case of the MCM-48-di (4.44 mmol N/g) compared to MCM-48-mono (1.77 mmol N/g). However, the N loading obtained for MCM-48-tri (4.85 mmol N/g) is only 10% larger compared to MCM-48-di (4.44 mmol N/g). This is due to a lower loading of the tri-amine silane (total weight loss in the 403-1073 K interval was 22.8%, compared to 21.7% for MCM-48-di), due to the steric effects experienced by this large molecule (length=1.65 nm) on the 3.5 nm pores of the MCM-48. The XRD analysis, see Figure 3, showed that functionalization caused an apparent loss of crystallinity when compared to the non-

functionalized MCM-48, especially in the case of the di-amino and tri-amino samples. Kim et al.<sup>28</sup> reported that the case of M41S family materials, the peak intensity is a function of the scattering contrast between the silica walls and the pore channels, and this intensity decreases after grafting the organic groups to the pore surface. Therefore, the decrease of the XRD peak intensity is probably due to the grafting the organic groups, rather than to a loss of structure. Similar changes have been reported with previous studies of functionalization of mesoporous silica.<sup>24,28</sup>

FTIR spectra of the samples are presented in Figure 5. The peak at the  $3743\text{ cm}^{-1}$  is assigned to single Si-OH, and this band completely disappeared in the functionalized MCM-48 samples, which indicates that all single Si-OH groups were covalently attached through siloxane Si-O-Si bonds with the silane agent. The grafting was also confirmed by the appearance of absorption peaks of N-H bonds ( $3368\text{-}3298\text{ cm}^{-1}$  and  $1590\text{-}1478\text{ cm}^{-1}$ ) and C-H bonds ( $2931\text{-}2869\text{ cm}^{-1}$ ) consistent with the functional groups used.<sup>28-30</sup>

#### *Dielectric Properties and microwave heating*

The dielectric constant ( $\epsilon'$ ), dielectric loss ( $\epsilon''$ ) and the loss tangent ( $\tan\delta$ ) are presented in Figure 6(a,b) as a function of temperature. 473 K was chosen as the maximum temperature for these tests following the results of the TGA analysis (see supplementary information) indicating that above this temperature a significant degradation of the functional groups could take place. Figure 6 shows that increasing the concentration of amino groups increased the dielectric constant and dielectric loss compared to non-functionalized MCM-48 samples. The increase in the dielectric constant is related to higher density of N-H dipoles (see Figure 1b, c) that can move freely in the grafted molecules. The loss tangent (Figure 6b), shows the efficiency of MW energy conversion into heat. In the case of MCM-48, this value decreases with

temperature in the entire interval studied. For this material, as the temperature increases, the condensation of the polar O-H groups on the silica surface takes place and after 100°C, most of them have disappeared and the value of loss tangent is negligible indicating that this material has a very low capacity to absorb microwave energy. However, in the case of the amino-grafted materials as the number of N-H groups increases, the loss tangent increases. The loss tangent values correlate perfectly with the heating experiments under microwave shown in Figure 7. In this experiment, three slabs of amino modified materials were placed together inside the microwave cavity, and the temperature of the surface of the slabs was recorded with an IR camera, (see Figure 7a). After the samples were allowed to reach a steady temperature, a clear temperature difference could be observed. The samples with lower amino group content and thus lower loss tangent presented the lowest temperature. The same effect could be observed by following the temperature inside a fixed-bed packed with the different powders and heated in the microwave cavity (Figure 7b). Again, the MCM-48-tri heated more intensely, reaching 413 K in 3 min, a temperature well above that required for the regeneration amino functionalized materials exposed to CO<sub>2</sub>, as will be shown below.

### *CO<sub>2</sub> adsorption*

Figure 8 shows CO<sub>2</sub> adsorption isotherms at 298 K for the different samples. As could be expected, for the same partial pressure the amount of CO<sub>2</sub> adsorbed increases as the density of amino groups increases. In the case of MCM-48-mono with an amine load of 1.77 mmol N/g a maximum CO<sub>2</sub> adsorption around 1 mmol CO<sub>2</sub>/g could be achieved, a value that agrees well with previous data on the same material.<sup>24</sup> In the case of MCM-48-di and tri, there a sharp increase in the isotherm can be observed at low partial pressure of CO<sub>2</sub>, corresponding to a Langmuir type I isotherm, indicating

that chemisorption takes place. For the MCM-48-di and tri samples a load around 0.3 mmol CO<sub>2</sub>/mmol N at 5kPa of CO<sub>2</sub> was achieved, see Table 1.

Chang et al.<sup>29</sup> reported that the reaction of CO<sub>2</sub> with amino groups under dry and humid conditions results in the formation of carbamates, giving a ratio of 0.5 mmol CO<sub>2</sub>/mmol N for -mono and -di and 0.66 mmol CO<sub>2</sub>/mmol N for -tri. This means that there is still considerable room for optimization of the grafting procedure in our samples that could lead to further increases in CO<sub>2</sub> loading.

#### *Thermal and microwave regeneration of sorbents*

The CO<sub>2</sub> desorption curves under conventional and microwave heating are presented in Figure 9(a,b), together with the evolution of temperature and normalized occupancy (Figure 9c) of the sorbent. The kinetic analysis<sup>19</sup> showed that, even though under conventional heating the highest available heating ramp was attempted (20K/min) desorption using microwave heating is approximately 4 times faster. Again, it can be seen that the MCM-48-tri sample present the fastest heating (and fastest) regeneration of the three amino-functionalized samples.

Finally, to test the stability and the regenerability of solid sorbents under microwave heating, a series of cyclic experiments involving CO<sub>2</sub> adsorption at room temperature and desorption under microwave heating were performed with mono-, di- and tri-amine functionalized MCM-48 samples (Figure 10). The average CO<sub>2</sub> uptakes in 20 cycles (except di-, only 8 cycles) for mono, di- and tri- amine functionalized samples were 0.2±0.02, 1.23±0.07 and 1.59 ± 0.10 mmol CO<sub>2</sub>/g sorbent, respectively. It can be seen that the stability was excellent, with no apparent loss of adsorption capacity after 20 cycles. The stability can be attributed to the chemical grafting of the amino groups on the silica surface, giving a clear advantage to these materials over amine-impregnated silica where amine leaching (and the subsequent loss of capacity) is

common.<sup>31</sup> With grafted molecules, the behavior is highly stable unless conditions are strong enough to break covalent bonds, giving covalently tethered amine adsorbents the potential to be subjected to repeated adsorption and desorption cycles<sup>32</sup> as shown in Figure 10.

## **Conclusions**

The dielectric characterization measurements show that the incorporation of amino groups on otherwise low-interaction supports such as silica, enables polarization by the electromagnetic field and strongly enhances response in the microwave frequency range. This results in direct heating of the surface of amino-grafted silica, accelerating temperatures rise and desorption of adsorbed species. The advantages for sorbent regeneration are substantial since energy is directly transferred to the solid in a highly efficient way, and also because the accelerated desorption facilitates the production of a highly concentrated exit stream.

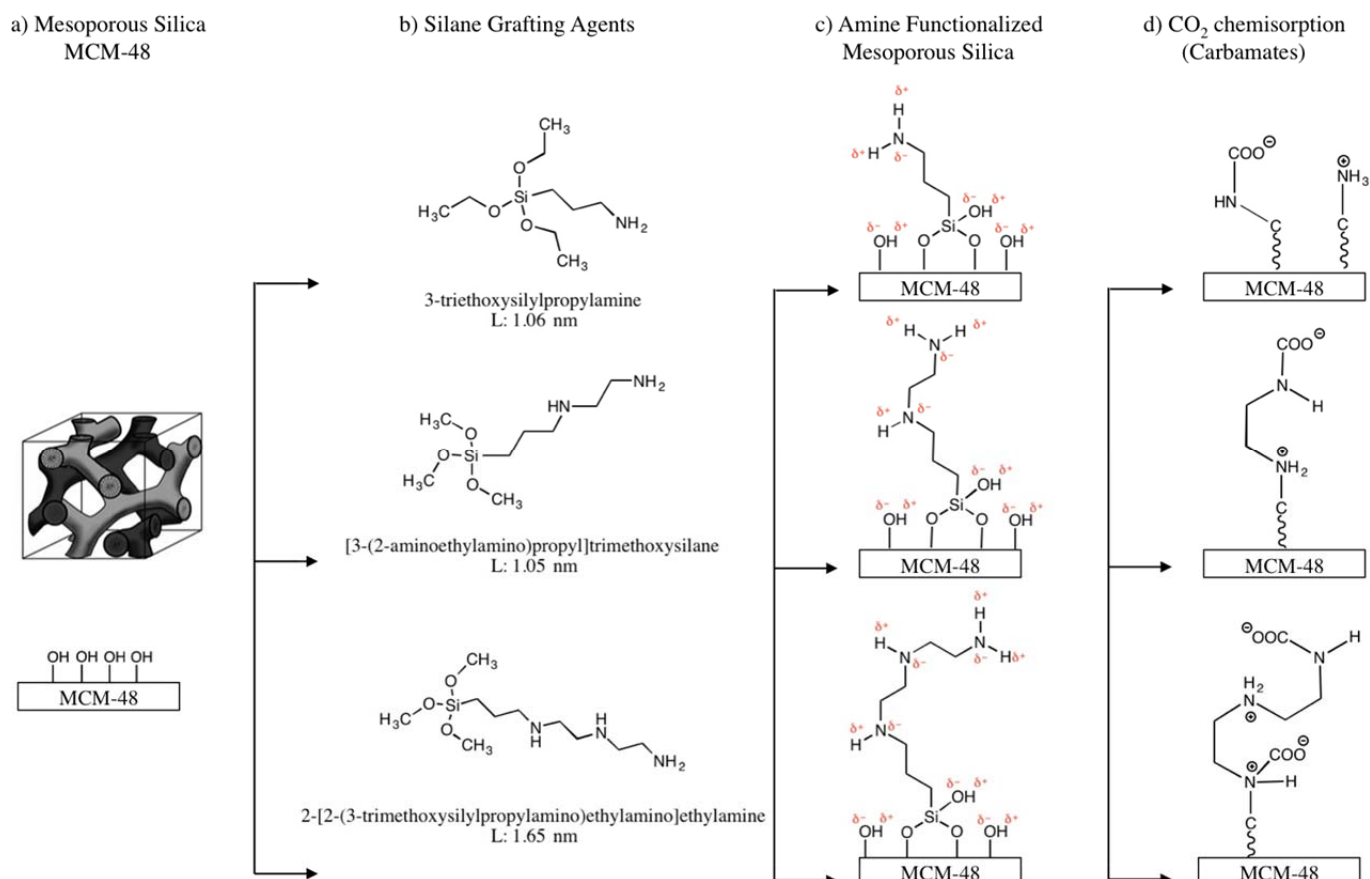
The MWSA process using amino-functionalized materials seems especially apt for CO<sub>2</sub> capture systems. Increasing the concentration of amino groups (by grafting mono, di- and tri-amine molecules) simultaneously increases CO<sub>2</sub> adsorption at low ambient partial pressures and the response under MW heating at 2.45 GHz, leading to a fast (approximately 4 times faster than conventional heating under the conditions studied) regeneration. Furthermore, chemical grafting produces a stable material under MWSA conditions: no effect was observed on the adsorption capacity after 20 adsorption-regeneration cycles.

### *Acknowledgments*

Financial support from the European Research Council ERC-Advanced Grant HECTOR is gratefully acknowledged. Hakan Nigar also acknowledges financial support from the Spanish Ministry of Education for the FPU grant (Formación del Profesorado Universitario – FPU12/06864).

## FIGURES

Figure 1 – Schematic view of the covalent bonding through the alkyl-silyl linkages and formation of carbamates<sup>29</sup>.



- ChemDraw Professional v.15 was used for drawing the molecules.
- Schematized figure of MCM-48 was adapted from: Mesosilica materials and organic pollutant adsorption: part A removal from air , DOI: 10.1039/c3cs60096c

Figure 2 – TEM images of pristine MCM-48 sample after calcination

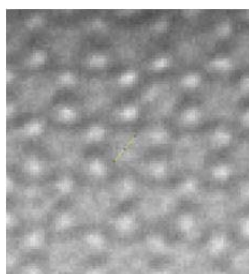
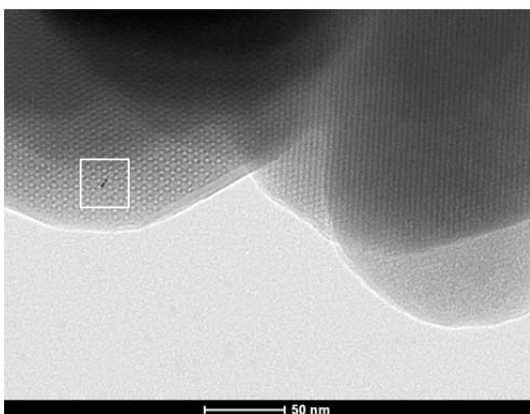
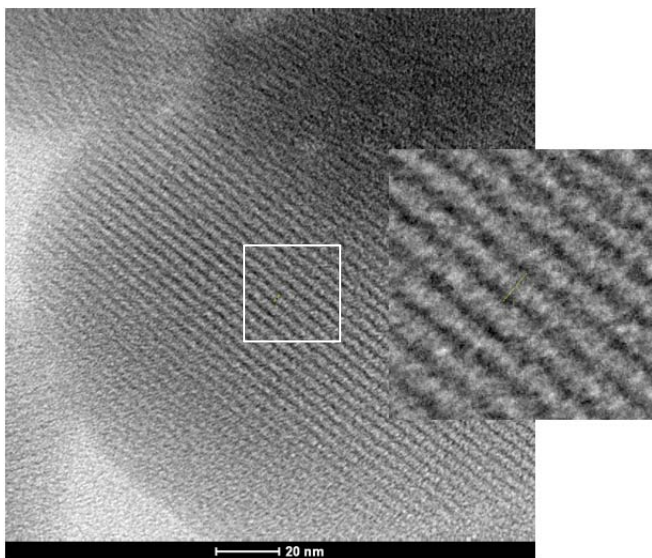


Figure 3 – XRD patterns of non-functionalized and functionalized MCM-48 samples

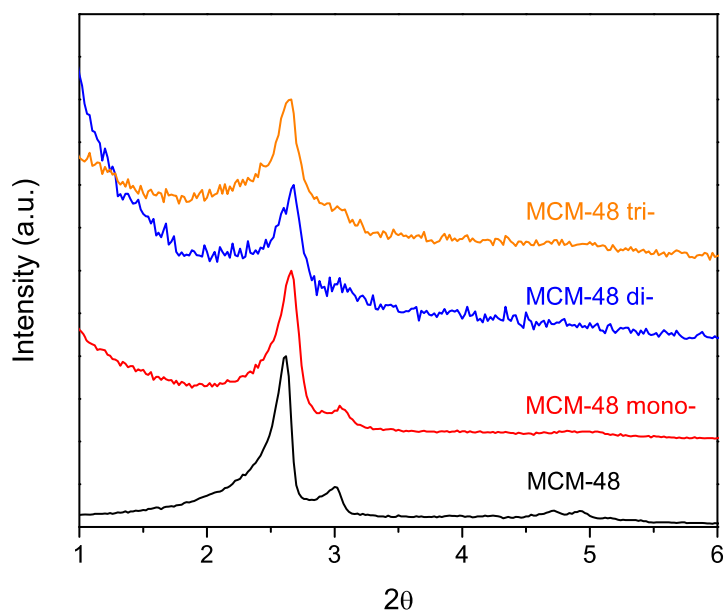
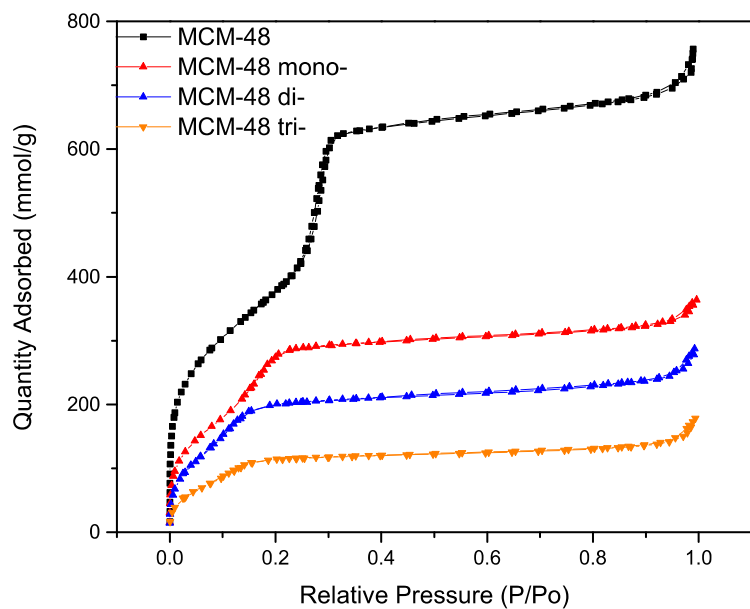


Figure 4 – (a) N<sub>2</sub> adsorption-desorption isotherms and (b) pores size distribution of non-functionalized and functionalized MCM-48 samples

a)



b)

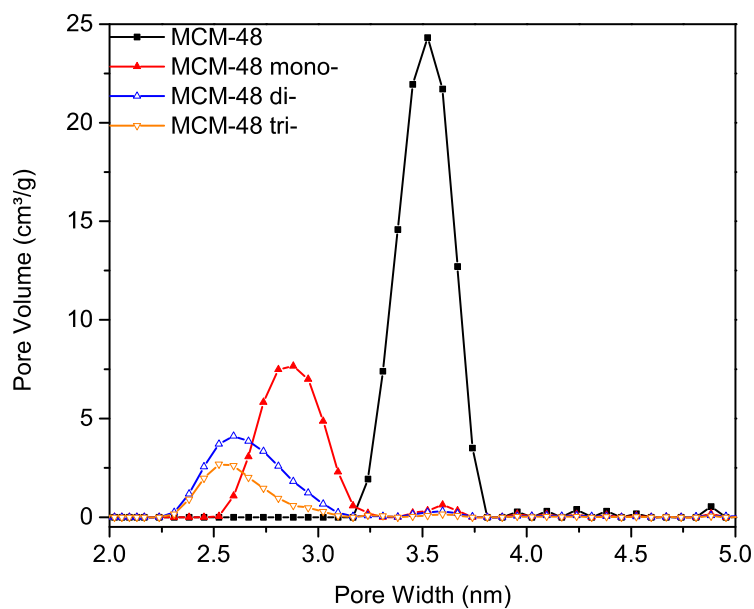


Figure 5 – FTIR spectrum of non-functionalized and functionalized MCM-48 samples

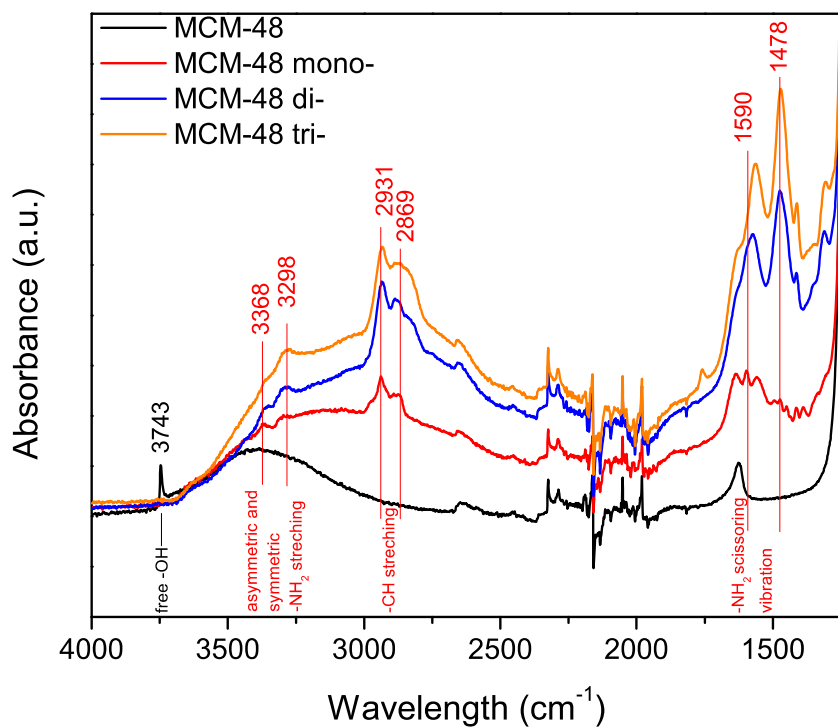
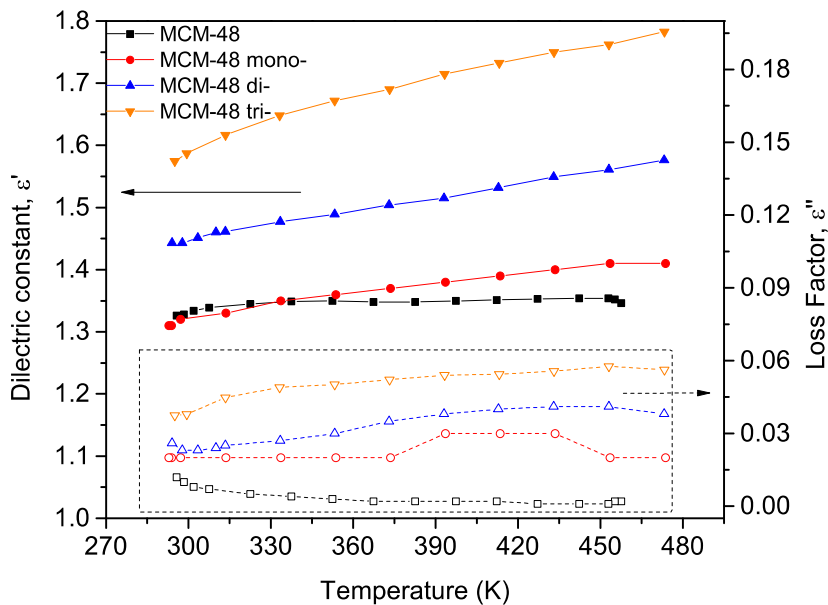


Figure 6 – Dielectric Properties, a) dielectric constant and loss factor, b) loss tangent as a function of temperature

a)



b)

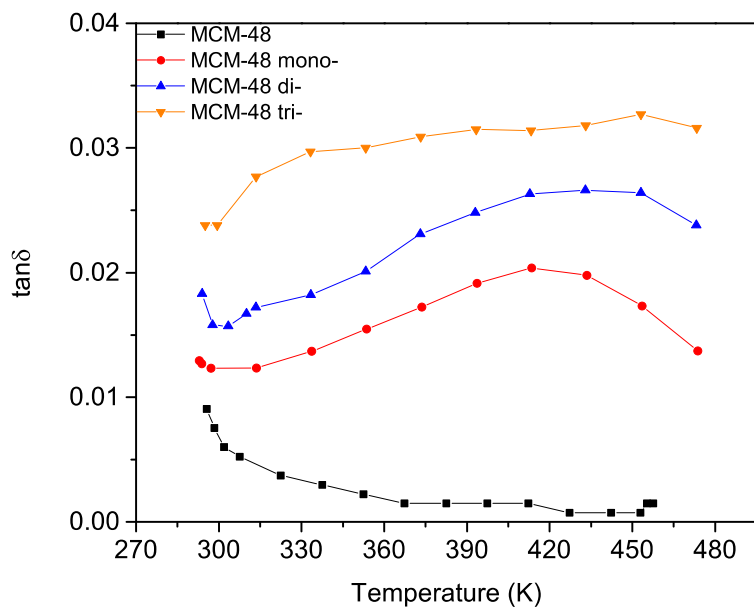


Figure 7 – a) Surface temperature, measure with thermographic camera of functionalized samples heated inside the MW cavit, 5W. b) Temperature vs. time in fixed-bed of the different samples, m=100 mg, 60W. Temperature measured with an optical fiber located inside the bed

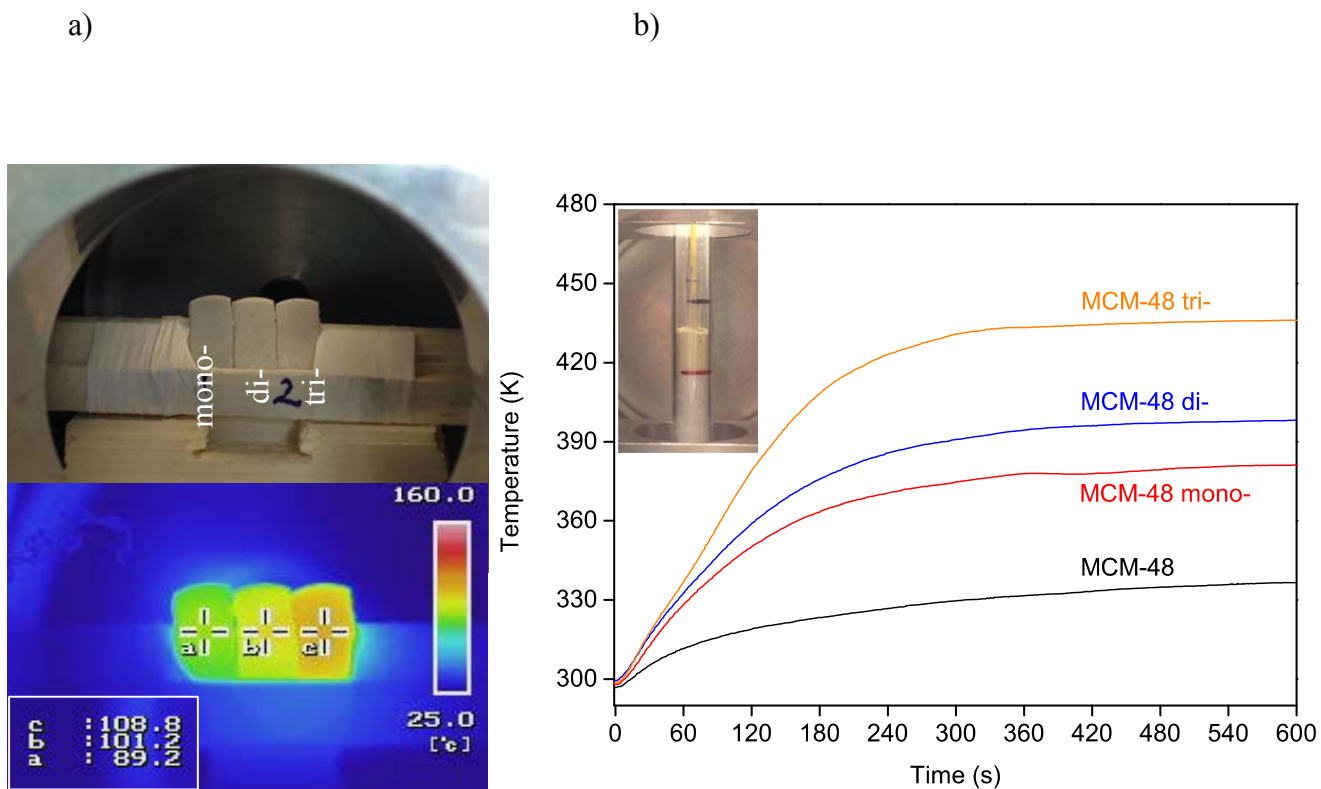


Figure 8 – CO<sub>2</sub> adsorption isotherms at 298 K for non-functionalized and functionalized MCM-48 samples

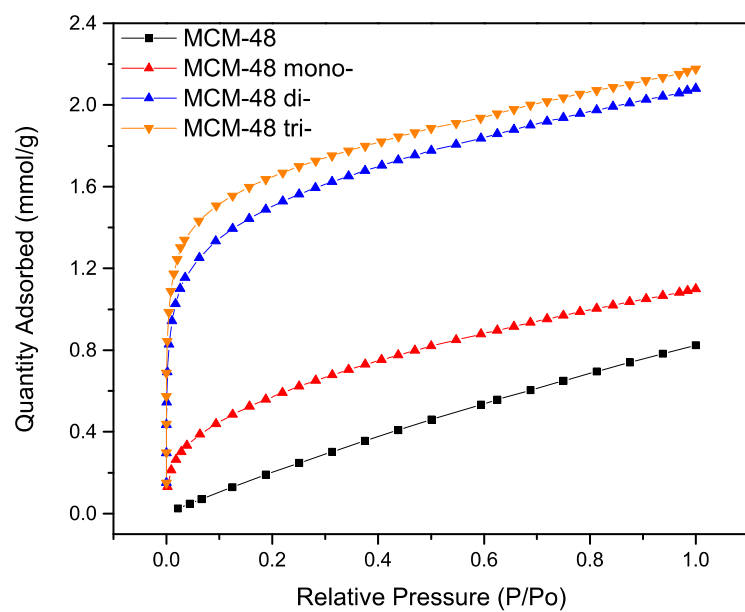
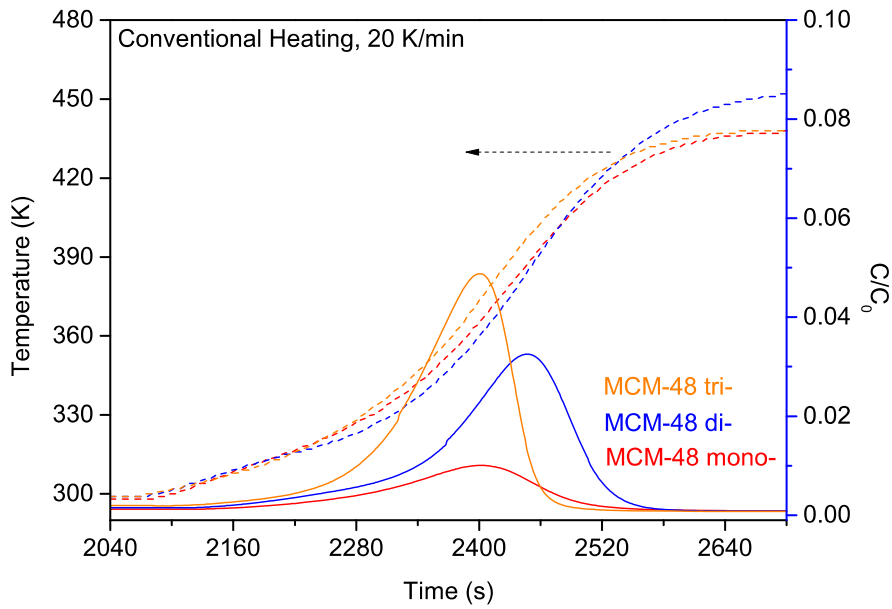
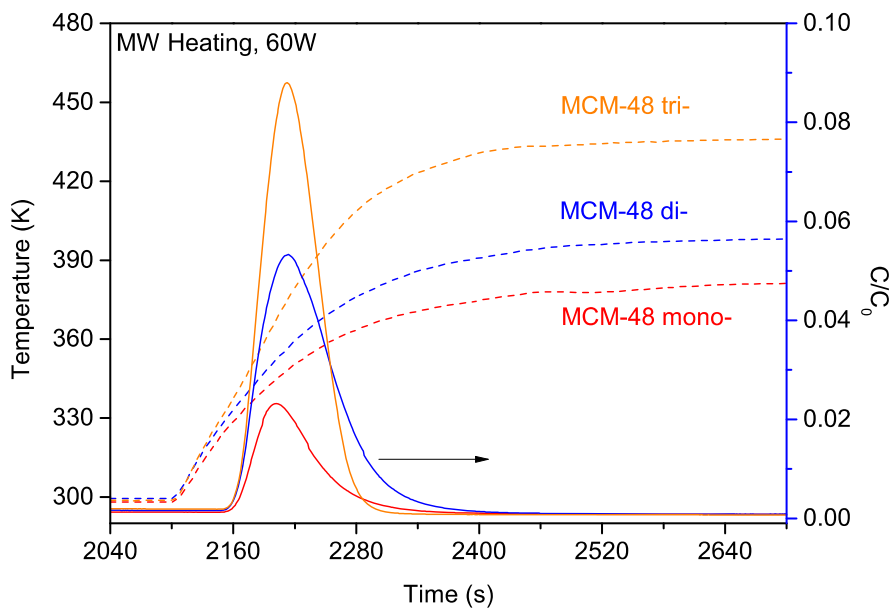


Figure 9 – Evolution of temperature and normalized concentration during a) conventional and b) MW regeneration of sorbents saturated with CO<sub>2</sub> at 1 bar 298 K. c) Occupancy vs. Time for conventional and MW heating

a)



b)



c)

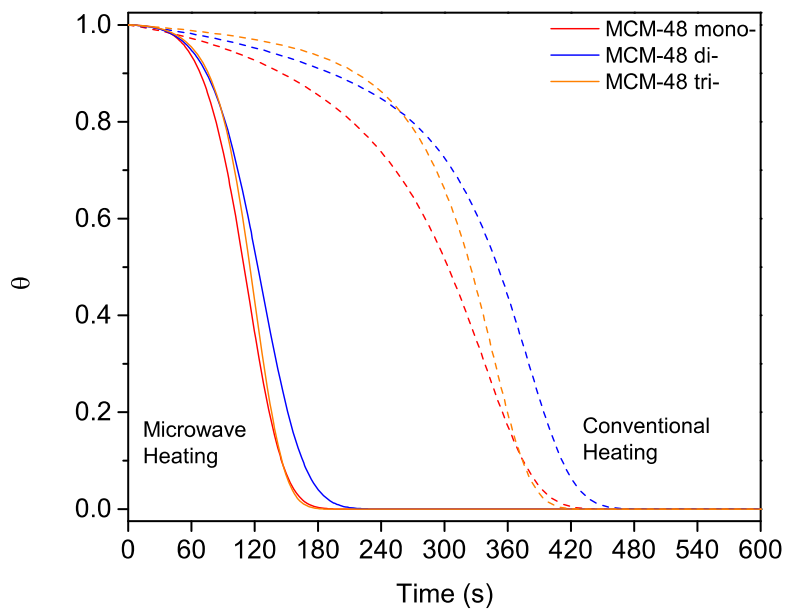
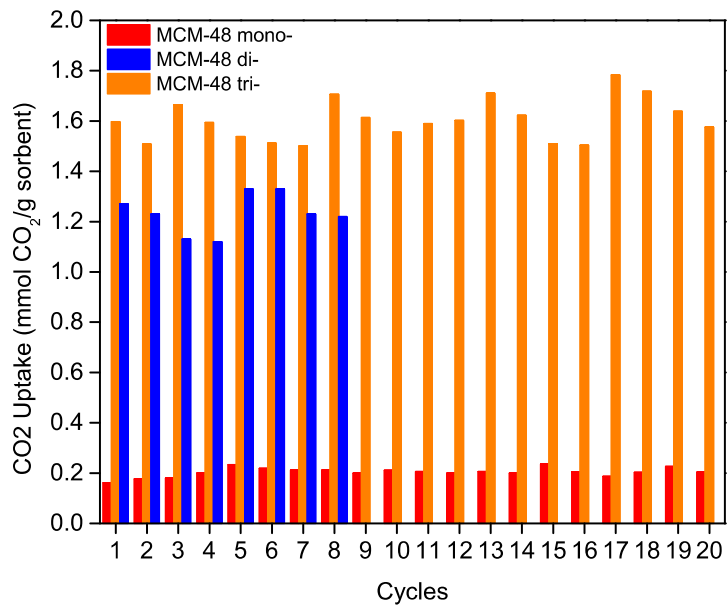


Figure 10 – Cyclic adsorption of CO<sub>2</sub>



TABLES

Table 1 – Textural properties and CO<sub>2</sub> uptake extracted from N<sub>2</sub> and CO<sub>2</sub> isotherms of MCM-48 samples with varying degrees of amine functionalization

| Sample       | BET<br>Surface<br>Area | Pore<br>Volume     | Pore<br>Size | mmol<br>N/g | mmol CO <sub>2</sub> /<br>mmol N<br>@5 kPa | mmol CO <sub>2</sub> /<br>mmol N<br>@101 kPa |
|--------------|------------------------|--------------------|--------------|-------------|--|--|
|              | m <sup>2</sup> /g      | cm <sup>3</sup> /g | nm           |             |  |  |
| MCM-48       | 1287                   | 1.11               | 3.5          | -           | -  | -  |
| MCM-48 mono- | 1072                   | 0.52               | 2.9          | 1.77        | 0.22                                       | 0.62   |
| MCM-48 di-   | 698                    | 0.39               | 2.6          | 4.44        | 0.27                                       | 0.46   |
| MCM-48 tri-  | 463                    | 0.23               | 2.5          | 4.85        | 0.31                                       | 0.44   |

## REFERENCES

1. Boot-Handford ME, Abanades JC, Anthony EJ, et al. Carbon capture and storage update. *Energy and Environmental Science*. 2014;7(1):130-189.
2. Goeppert A, Czaun M, Surya Prakash GK, Olah GA. Air as the renewable carbon source of the future: An overview of CO<sub>2</sub> capture from the atmosphere. *Energy and Environmental Science*. 2012;5(7):7833-7853.
3. Mason JA, Sumida K, Herm ZR, Krishna R, Long JR. Evaluating metal-organic frameworks for post-combustion carbon dioxide capture via temperature swing adsorption. *Energy and Environmental Science*. 2011;4(8):3030-3040.
4. Harlick PJE, Sayari A. Applications of pore-expanded mesoporous silica. 5. triamine grafted material with exceptional CO<sub>2</sub> dynamic and equilibrium adsorption performance. *Industrial and Engineering Chemistry Research*. 2007;46(2):446-458.
5. Franchi RS, Harlick PJE, Sayari A. Applications of pore-expanded mesoporous silica. 2. Development of a high-capacity, water-tolerant adsorbent for CO<sub>2</sub>. *Industrial and Engineering Chemistry Research*. 2005;44(21):8007-8013.
6. Webley PA, Zhang J. Microwave assisted vacuum regeneration for CO<sub>2</sub> capture from wet flue gas. *Adsorption*. 2014;20(1):201-210.
7. Stankiewicz A. On the Applications of Alternative Energy Forms and Transfer Mechanisms in Microprocessing Systems. *Industrial & Engineering Chemistry Research*. 2007/06/01 2007;46(12):4232-4235.
8. Clark DE, Folz DC, West JK. Processing materials with microwave energy. *Materials Science and Engineering: A*. 8/15/ 2000;287(2):153-158.
9. Chandrasekaran S, Ramanathan S, Basak T. Microwave material processing-a review. *AIChE Journal*. 2012;58(2):330-363.
10. Borrell A, Salvador MD, Miranda M, Penaranda-Foix FL, Catala-Civera JM. Microwave technique: A powerful tool for sintering ceramic materials. *Current Nanoscience*. 2014;10(1):32-35.
11. Durka T, van Gerven T, Stankiewicz A. Microwaves in heterogeneous gas-phase catalysis: Experimental and numerical approaches. *Chemical Engineering and Technology*. 2009;32(9):1301-1312.
12. Cherbański R, Molga E. Intensification of desorption processes by use of microwaves-An overview of possible applications and industrial perspectives. *Chemical Engineering and Processing: Process Intensification*. // 2009;48(1):48-58.
13. Hashisho Z, Rood MJ, Barot S, Bernhard J. Role of functional groups on the microwave attenuation and electric resistivity of activated carbon fiber cloth. *Carbon*. 2009;47(7):1814-1823.
14. Menéndez JA, Arenillas A, Fidalgo B, et al. Microwave heating processes involving carbon materials. *Fuel Processing Technology*. 1// 2010;91(1):1-8.
15. Çalışkan E, Bermúdez JM, Parra JB, Menéndez JA, Mahramanlioğlu M, Ania CO. Low temperature regeneration of activated carbons using microwaves: Revising conventional wisdom. *Journal of Environmental Management*. 2012;102:134-140.

16. Ohgushi T, Komarneni S, Bhalla AS. Mechanism of microwave heating of zeolite A. *Journal of Porous Materials*. 2001;8(1):23-35.
17. Legras B, Polaert I, Estel L, Thomas M. Mechanisms responsible for dielectric properties of various faujasites and linde type A zeolites in the microwave frequency range. *Journal of Physical Chemistry C*. // 2011;115(7):3090-3098.
18. Gracia J, Escuin M, Mallada R, Navascues N, Santamaría J. Heating of zeolites under microwave irradiation: A density functional theory approach to the ion movements responsible of the dielectric loss in Na, K, and Ca A-zeolites. *Journal of Physical Chemistry C*. // 2013;117(30):15659-15666.
19. Nigar H, Navascués N, De La Iglesia O, Mallada R, Santamaría J. Removal of VOCs at trace concentration levels from humid air by Microwave Swing Adsorption, kinetics and proper sorbent selection. *Separation and Purification Technology*. 2015;151:193-200.
20. Catala-Civera JM, Canos AJ, Plaza-Gonzalez P, Gutierrez JD, Garcia-Banos B, Penaranda-Foix FL. Dynamic Measurement of Dielectric Properties of Materials at High Temperature During Microwave Heating in a Dual Mode Cylindrical Cavity. *Microwave Theory and Techniques, IEEE Transactions on*. 2015;63(9):2905-2914.
21. Belmabkhout Y, Sayari A. Isothermal versus non-isothermal adsorption-desorption cycling of triamine-grafted pore-expanded MCM-41 mesoporous silica for CO<sub>2</sub> capture from flue gas. *Energy and Fuels*. 2010;24(9):5273-5280.
22. Chowdhury T, Shi M, Hashisho Z, Kuznicki SM. Indirect and direct microwave regeneration of Na-ETS-10. *Chemical Engineering Science*. 5/24/2013;95:27-32.
23. Chronopoulos T, Fernandez-Diez Y, Maroto-Valer MM, Ocone R, Reay DA. CO<sub>2</sub> desorption via microwave heating for post-combustion carbon capture. *Microporous and Mesoporous Materials*. 10// 2014;197:288-290.
24. Gil M, Tiscornia I, de la Iglesia Ó, Mallada R, Santamaría J. Monoamine-grafted MCM-48: An efficient material for CO<sub>2</sub> removal at low partial pressures. *Chemical Engineering Journal*. // 2011;175(1):291-297.
25. Sayari A, Heydari-Gorji A, Yang Y. CO<sub>2</sub>-induced degradation of amine-containing adsorbents: Reaction products and pathways. *Journal of the American Chemical Society*. 2012;134(33):13834-13842.
26. Jaroniec M, Kruk M, Olivier JP, Koch S. A new method for the accurate pore size analysis of MCM-41 and other silica based mesoporous materials. *Studies in Surface Science and Catalysis*. Vol 1282000:71-80.
27. Schumacher K, Ravikovitch PI, Du Chesne A, Neimark AV, Unger KK. Characterization of MCM-48 Materials. *Langmuir : the ACS journal of surfaces and colloids*. 2000/05/01 2000;16(10):4648-4654.
28. Kim S, Ida J, Gulians VV, Lin JYS. Tailoring pore properties of MCM-48 silica for selective adsorption of CO<sub>2</sub>. *Journal of Physical Chemistry B*. 2005;109(13):6287-6293.
29. Chang F-Y, Chao K-J, Cheng H-H, Tan C-S. Adsorption of CO<sub>2</sub> onto amine-grafted mesoporous silicas. *Separation and Purification Technology*. 11/19/2009;70(1):87-95.
30. Bacsik Z, Ahlsten N, Ziadi A, et al. Mechanisms and kinetics for sorption of CO<sub>2</sub> on bicontinuous mesoporous silica modified with n-propylamine. *Langmuir : the ACS journal of surfaces and colloids*. Sep 6 2011;27(17):11118-11128.

31. Chen C, Yang S-T, Ahn W-S, Ryoo R. Amine-impregnated silica monolith with a hierarchical pore structure: enhancement of CO<sub>2</sub> capture capacity. *Chemical Communications*. 2009(24):3627-3629.
32. Choi S, Drese JH, Jones CW. Adsorbent Materials for Carbon Dioxide Capture from Large Anthropogenic Point Sources. *ChemSusChem*. 2009;2(9):796-854.